Random matrix model at nonzero chemical potentials with anomaly effects

H. Fujii[1] and T. Sano[1,2]

[1]*Institute of Physics, The University of Tokyo, Tokyo 153-8902, Japan*
[2]*Department of Physics, The University of Tokyo, Tokyo 113-0033, Japan*
(Received 6 October 2010; published 13 January 2011)

Phase diagram of the chiral random matrix model with $U(1)_A$ breaking term is studied with the quark chemical potentials varied independently at zero temperature by taking the chiral and meson condensates as the order parameters. Although, without the $U(1)_A$ breaking term, chiral transition of each flavor can happen separately responding to its chemical potential, the $U(1)_A$ breaking terms mix the chiral condensates and correlate the phase transitions. In the three-flavor case, we find that there are mixings between the meson and chiral condensates due to the $U(1)_A$ anomaly, which makes the meson condensed phase more stable. Increasing the hypercharge chemical potential (μ_Y) with the isospin and quark chemical potentials (μ_I, μ_q) kept small, we observe that the kaon-condensed phase becomes the ground state and at the larger μ_Y the pion-condensed phase appears unexpectedly, which is caused by the competition between the chiral restoration and the meson condensation. The similar happens when μ_Y and μ_I are exchanged, and the kaon-condensed phase becomes the ground state at larger μ_I below the full chiral restoration.

I. INTRODUCTION

The phase diagram of QCD at finite density has long been challenged from the perspectives on the fundamental properties of dense matter realized in the core of a compact star and relativistic heavy-ion collisions. The chiral symmetry breaking in light quark sector is one of the crucial features in low-energy QCD which should be reflected in any effective model. In the massless quark limit with flavor number $N_f = 2$ or 3, chiral symmetry breaking gives rise to continuously degenerate vacua and to emergence of the massless Nambu-Goldstone bosons as the most important degrees at low energies. In reality, nonzero u- and d-quark masses and heavier s-quark mass lift this degeneracy and explain the observed pseudoscalar meson spectrum.

A system at finite quark number densities is characterized with the quark number chemical potentials μ_f ($f =$ u, d, s) in the grand canonical description. The simplest situation at finite density may be the case with equal chemical potentials $\mu = \mu_u = \mu_d = \mu_s$ for all flavors, where the s-quark density may be suppressed compared with the u and d quarks due to the mass difference. However, the quark chemical potentials μ_f are generally unequal in various physical situations. There are more protons than neutrons in nuclei and also in neutron stars because of the electric charge of protons. In the core of compact stars in beta equilibrium, the heavy mass of the s quark may be overcome by the large electric chemical potential, which may result in the appearance of s-quark degrees of freedom. In ultrarelativistic heavy-ion collisions the total strangeness number is constrained to zero.

The phase structure at finite chemical potentials has very rich theoretical possibilities [1–4]. Historically, in dense nuclear matter, nucleon superfluidity, pion and kaon condensations, and hyperon mixture were studied based on empirical nucleon interactions and chiral perturbation theory [3]. More recently, color superconductivity was extensively investigated and the kaon-condensed phase acquired renewed interests there [4]. Possibility of inhomogeneous phases is also discussed recently[1] [5].

Another motivation to consider the phase diagram with unequal chemical potentials is that one can directly examine in lattice QCD simulations the $N_f = 2$ case with finite isospin and zero quark chemical potentials, $\mu_I \equiv (\mu_u - \mu_d)/2 \neq 0$ and $\mu_q \equiv (\mu_u + \mu_d)/2 = 0$, where the measure for the importance sampling is real. We note that it may be possible to simulate the $N_f = 3$ case with $\mu_I \neq 0$ and $\mu_q = \mu_s = 0$, at least in principle.

The ground state at finite isospin chemical potential but at zero quark number density was studied with the chiral Lagrangian, which revealed that the pion condensate appears once μ_I exceeds half the pion mass $m_\pi/2$ [6]. Indeed, in the chiral limit, the degenerate ground state is completely chiral-rotated to the pion-condensed state at infinitesimal external field $\mu_I \neq 0$. Adding a finite quark mass $m_q \neq 0$, which makes the pion massive, we have a competition between the two alignments, $\langle \bar{q}q \rangle$ and $\langle \bar{u}\gamma_5 d \rangle$ directions for m_q and μ_I, respectively. In the three-flavor case, kaon condensation appears once the hypercharge chemical potential μ_Y exceeds the threshold given by m_K with $\mu_I = 0$ [7].

The chiral random matrix (ChRM) model is one of the models which share the chiral symmetry with QCD. Thus,

---

[1]The *p*-wave pion-condensed phase too accompanies inhomogeneity [3].

it will serve as a useful model providing qualitative features of the QCD phase diagram. The aim of this paper is to explore the phase structure of the (ChRM) model, including the possibilities of the meson condensations, as a function of the quark chemical potentials μ_f (f = u, d, s) at zero temperature.

In the previous work of the ChRM model with two flavors done in Ref. [8], it was shown that the pion-condensed phase appears at finite μ_I above a critical value μ_{Ic} as suggested by [6], whereas it eventually disappears as μ_I is further increased, which is understood as the chiral restoration at high density. It was also indicated that with small nonzero μ_I the chiral restoration occurs in two steps: as μ_q is increased with (e.g.) negative $\mu_I < 0$ fixed, the $\langle \bar{d}d \rangle$ condensate discontinuously decreases first, and then the $\langle \bar{u}u \rangle$ at slightly larger μ_q. The two- (or three-) step transition along the μ_q axis with finite μ_I and/or μ_Y is also observed in the three-flavor case of the ChRM model [9,10] and in the two and three-flavor cases of the Nambu–Jona-Lasinio (NJL) model [11–14].

This two-step transition happens evidently because these models do not include flavor mixing interactions and then each quark sector independently responds to each quark chemical potential μ_f. The U(1)$_A$ anomaly in QCD is known to induce the flavor mixing and tends to unify the two chiral transitions into one. This is demonstrated in the NJL model with U(1)$_A$ breaking effective interactions, which results in the usual phase diagram with a single transition [14].

The U(1)$_A$ anomaly effect is indispensable to build a low-energy effective model of hadrons in medium as well as in vacuum [15–17]. Although in a conventional ChRM model the U(1)$_A$ anomaly effect is not treated appropriately so as to affect the nature of the chiral transition, recently we have succeeded in constructing the model in which the U(1)$_A$ breaking term generates the flavor-number dependence of the transition order [18]. This model in the massless quark limit shows the second-order phase transition for $N_f = 2$, whereas the first-order one for $N_f = 3$. We explored the phase diagram of the model in the T–μ_q–m_q space with $\langle \bar{q}_f q_f \rangle$ as the order parameter [19].

It seems now quite intriguing to investigate the phase diagram allowing the pion and kaon condensates in the ChRM model with $N_f = 2$ and 3 as a function of the chemical potentials μ_f, with emphasis on the role of the U(1)$_A$ anomaly. Similar studies were previously performed employing the NJL model with U(1)$_A$ anomaly effects [14,20,21]. In Ref. [14], the phase structure for $N_f = 2$ is studied only in small μ_I region below the threshold for the pion condensation, and the study is extended by including the pion-condensed phase in Ref. [20]. Ref. [21] deals with the $N_f = 3$ case restricted at $\mu_I \neq 0$ and $\mu_Y = 0$, where the possibility of kaon condensation is ignored.

This paper is organized as follows. After a review of the QCD phase structure with finite chemical potentials in Sec. II, we introduce the ChRM model with anomaly effects in Sec. III. The model phase structure including the possibility of the mesonic condensation is investigated analytically and numerically in Secs. IV and V for $N_f = 2$ and 3, respectively. Sec. VI is devoted to a summary.

II. QCD WITH QUARK CHEMICAL POTENTIALS

In this section, we briefly review the symmetry breaking pattern of QCD with nonzero quark chemical potentials. The QCD partition function with N_f quark flavors at finite temperature and chemical potential is regarded as the average of the Dirac operators with non-Abelian gauge field action S_{YM}:

$$Z_{QCD} = \int \mathcal{D}A \prod_f^{N_f} \det(D(\mu_f) + m_f)e^{-S_{YM}}, \quad (1)$$

where $D(\mu_f) = \gamma_\nu(\partial_\nu - igA_\nu + B_\nu \mu_f)$ is the (Euclidean) Dirac operator for a flavor f and m_f is the mass. The quark number chemical potential μ_f is introduced independently for each quark flavor f with a constant Lorentz vector $B_\nu = (0, 0, 0, 1)$.

In the massless limit $m_f = 0$ with zero chemical potential $\mu_f = 0$, the classical QCD Lagrangian possesses U(N_f)$_L$ × U(N_f)$_R$ chiral symmetry, which is broken down to U(1)$_B$ × SU(N_f)$_L$ × SU(N_f)$_R$ at the quantum level due to the axial anomaly. The $U(1)_B$ invariance results in the quark number conservation. Nonperturbative QCD dynamics is believed to break this symmetry spontaneously to U(1)$_B$ × SU(N_f)$_V$, generating a large part of the nucleon mass and the light pions as the Nambu-Goldstone (NG) boson. In reality, nonzero quark mass term acts as an external field to select the ordinary vacuum state with nonzero $\langle \bar{q}q \rangle$ condensate out of the nearly degenerate vacua.

The chiral symmetry of QCD is intact at finite quark number chemical potential as far as it is flavor singlet, which is usually assumed in the context of finite density QCD. Once the flavor-nonsinglet potential is set nonzero, it gives a stress on the flavor symmetric ground state in addition to the quark mass term. Symmetry breaking pattern in this situation has been studied most conveniently with the chiral Lagrangian [6,7].

Let us consider the $N_f = 2$ case with the small u- and d-quark masses $m_u = m_d$. At zero chemical potential there appear nearly degenerate vacua connected with each other by the SU(2) × SU(2) ≃ O(4) transformation, and the true ground state aligns to the direction of the quark mass term with SU(2)$_V$ invariance. When the isospin chemical potential $\mu_I = (\mu_u - \mu_d)/2$ is applied, this invariance explicitly breaks down to U(1) ∈ SU(2)$_V$ around the 3rd isospin axis. The mass m and the potential μ_I compete to fix the ground state. For $\mu_I > m_\pi/2$, a new class of the degenerate vacua appears with nonzero pion field and the ground

state spontaneously breaks the U(1) symmetry, which is accompanied by the appearance of an NG boson. This symmetry breaking pattern is summarized as follows:

$$U(1)_B \times SU(2)_V \overset{\mu_I \neq 0}{\to} U(1)_B \times U(1) \overset{\pi^c \, \text{cond}}{\to} U(1)_B. \quad (2)$$

For $N_f = 3$, we consider the $2 + 1$ flavor case, where the quark masses $m_u = m_d \neq m_s$ and the chemical potentials $\mu_u \neq \mu_d \neq \mu_s$ in general. In this case, all flavor symmetry is broken explicitly leaving only $U(1) \times U(1) \times U(1)$ invariance, which represents the conservation of each flavor. Once (e.g.) $\bar{d}\gamma_5 s$ meson condensate is formed in addition to the nonzero chiral condensates, the symmetry is spontaneously broken down to $U(1) \times U(1)_{ds}$, where $U(1)_{ds}$ leaves the condensate $\langle \bar{d}\gamma_5 s \rangle$ invariant. We also find one NG mode corresponding to the spontaneous breaking of U(1).[2] The symmetry breaking pattern is

$$U(1)_B \times SU(3)_V \overset{\mu_f \neq 0}{\to} U(1) \times U(1)$$
$$\times U(1) \overset{K \, \text{cond}}{\to} U(1) \times U(1)_{ds}. \quad (3)$$

III. RANDOM MATRIX MODEL

The chiral random matrix model [24,25] is constructed based on the idea that the spontaneous breaking of the chiral symmetry is dominated by the low-lying Dirac eigenmodes, as is manifest in the Banks-Casher relation between the chiral condensate and the spectral density near zero [26]. The Dirac operator D is then truncated to be a matrix within the restricted space spanned by the (quasi-) zero modes, and the matrix elements are treated as random variables. Explicitly, in the representation where $\gamma_5 = \text{diag}(1, -1)$, we have

$$D = \begin{pmatrix} 0 & iR + C \\ iR^\dagger + C^T & 0 \end{pmatrix}, \quad (4)$$

where R is a rectangular complex random matrix and C is a nonrandom matrix responsible for the effects of temperature and chemical potentials. Note that the block structure follows from the chiral symmetry $\{\gamma_5, D\} = 0$.

When the matrix R is not square but rectangular, the Dirac operator D has $|\nu|$ exact zero eigenvalues with $|\nu|$ being the difference between the numbers of the rows and the columns of R. This is the realization of the index theorem for the topological charge and the number of exact zero modes in ChRM model. Hence, in order to include the anomaly effects, we need to deal with the nonsquare matrix properly. To this end, we categorize the zero modes into two species, the near-zero modes and the topological zero modes [18]. The former are assumed to be N left- and N right-handed low-lying modes generated in gluon

dynamics, while the latter are interpreted as the modes, each of which is localized near one of N_+ instantons or N_- anti-instantons in a gauge field configuration. Then the size of the matrix R is taken as $(N + N_+) \times (N + N_-)$, and the topological charge of the configuration is $\nu = N_+ - N_-$. We take the number of the near-zero modes $2N$ and the mean number of the topological zero modes $\langle N_\pm \rangle$ to be proportional to the four-volume V of the system.

Concerning the matrix C, which represents the medium effects, we introduce the effective temperature T and chemical potential μ_f for a flavor f in the near-zero mode sector, while they are set to zero in the topological zero mode sector [18,25]:

$$C_f = \begin{pmatrix} (\mu_f + iT)\mathbf{1}_{N/2} & 0 & 0 \\ 0 & (\mu_f - iT)\mathbf{1}_{N/2} & 0 \\ 0 & 0 & 0 \end{pmatrix}. \quad (5)$$

In the near-zero mode sector, $\mu_f \pm iT$ may be interpreted as the contributions from the two lowest Matsubara frequencies. The Dirac operator D with nonzero chemical potential $\mu_f \neq 0$ is no longer antihermitian, though the partition function is invariant under $\mu_f \leftrightarrow -\mu_f$. We stress here the fact that the absence of the medium effects in the topological zero mode sector resolves the unphysical suppression of the topological susceptibility of the original ChRM model (see discussion in [27,28]). This form of C_f may be understood physically as the fact that a topological zero mode localized near an (anti-) instanton is rather insensitive to the medium effects.

Using the Dirac operator (4), we define the partition function of the ChRM model with fixed N_+ and N_- as

$$Z_{N_+,N_-} = \int dR \, e^{-N\Sigma^2 \text{tr}RR^\dagger} \prod_{f=1}^{N_f} \det(D(\mu_f) + m_f), \quad (6)$$

with a Gaussian weight for the matrix R. The typical scale of the chiral symmetry breaking is fixed by the parameter Σ. The complete partition function is obtained by summing over the numbers of topological zero modes N_+ and N_- with a distribution function $P(N_\pm)$ as

$$Z^{RM} = \sum_{N_+,N_-} P(N_+)P(N_-)Z_{N_+,N_-}. \quad (7)$$

The Poisson distribution would be appropriate for $P(N_\pm)$ in a dilute instanton system [16]. Adopting the Poisson distribution, however, one finds that the effective potential becomes unbounded from below [29]. Instead, we choose $P(N_\pm)$ to be a binomial distribution [18]

$$P(N_\pm) = \binom{\gamma N}{N_\pm} p^{N_\pm}(1-p)^{\gamma N - N_\pm} \quad (8)$$

with parameters γ and p. The binomial distribution models the situation that if we divide the four-volume V into γN cells, an instanton appears in one of the cells with the probability p, barring double occupancy. In other words,

---

[2]It is known that the numbers of the broken generators and the NG bosons can differ in some cases, e.g., feromagnetism, kaon-condensed phase with $\mu_I = 0$, etc. [22,23].

we introduced a repulsive interaction among instantons. This modification results in a bounded effective potential with a stable ground state [18].

After the standard bosonization manipulation, we can express the partition function at $T = 0$ as

$$Z^{\mathrm{RM}}(\mathcal{M}, \hat{\mu}) = \int dS e^{-2N\Omega} \qquad (9)$$

with the effective potential

$$\Omega(S; \mathcal{M}, \hat{\mu}) = \frac{\Sigma^2}{2} \operatorname{tr} S^\dagger S$$
$$- \frac{1}{2} \operatorname{logdet} \begin{bmatrix} S + \mathcal{M} & \hat{\mu} \\ \hat{\mu} & S^\dagger + \mathcal{M}^\dagger \end{bmatrix}$$
$$- \frac{\gamma}{2} \log |\alpha \det(S + \mathcal{M}) + 1|^2, \qquad (10)$$

where the bosonic field $S \in \mathbb{C}^{N_f \times N_f}$ is the order parameter matrix corresponding to the bifermion field $S_{fg} \sim \bar{\psi}_R^f \psi_L^g$, and $\mathcal{M} = \operatorname{diag}(m_u, m_d, \ldots, m_{N_f})$ and $\hat{\mu} = \operatorname{diag}(\mu_u, \mu_d, \ldots, \mu_{N_f})$ are the mass and the chemical potential matrices, respectively. The term involving the parameters γ and $\alpha = p/(1 - p)$ breaks the $U(1)_A$ symmetry $S \to Se^{i\theta}$ even in the $\mathcal{M} = 0$ limit [15,16]. In the thermodynamic limit, $N \to \infty$, the ground state is found as a solution of the saddle point equation $\partial \Omega / \partial S_{fg} = 0$. Using the solution $\bar{S}$, the chiral condensate can be computed for a flavor f as

$$\langle \bar{\psi}_f \psi_f \rangle = \frac{\partial}{\partial m_f} \Omega(\bar{S}; \mathcal{M}, \hat{\mu}) = -\Sigma^2 \bar{S}_{ff}. \qquad (11)$$

By generalizing the mass matrix to the source matrix $\mathcal{M} = (s^a + i p^a) \lambda^a / \sqrt{2}$ with the generators λ^a normalized $\operatorname{tr}(\lambda^a \lambda^b) = 2\delta^{ab}$, other scalar (chiral) and pseudoscalar (meson) condensates are evaluated by differentiating in s^a and p^a, respectively.

In the preceding works [18,19], we have studied the ground state of this model for $N_f = 2$ and 3 at finite temperature T and equal chemical potential μ. Regarding the anomaly parameters α and γ, we have found that, for the large anomaly parameters $\alpha\gamma \gtrsim \Sigma^2$, this model does not show chiral restoration, and therefore we should use the anomaly parameters in the region which allows the chiral phase transition. In the chiral limit, the chiral phase transition at finite T and zero μ is found to be second (first) order for $N_f = 2$ (3). This flavor-number dependence comes from the $U(1)_A$ anomaly term. Extending to the $\mu \neq 0$ case, we find that the transition on the $T-\mu$ plane changes from the second order to the first order at a tricritical point as μ is increased in the $N_f = 2$ case. For $N_f = 3$, the first-order phase boundary separates the $T-\mu$ plane into two regions. With increasing the quark mass, the thermal transition gets weakened and eventually turns to a smooth crossover, while the transition at larger μ than a

critical point remains of first order. Then the $T-\mu$ phase diagram becomes similar to the $N_f = 2$ case with small quark masses. For more detailed discussions, see Refs. [18,19].

IV. PHASE DIAGRAM: $N_f = 2$ CASE

A. Effective potential

We study the situation where $\mu_u \neq \mu_d$ with the degenerated quark masses $m_u = m_d \equiv m$. It is convenient to define the (averaged) quark chemical potential μ_q and the isospin chemical potential μ_I as

$$\mu_q = \frac{1}{2}(\mu_u + \mu_d), \qquad (12)$$

$$\mu_I = \frac{1}{2}(\mu_u - \mu_d). \qquad (13)$$

The order parameter matrix can be parametrized as $S = \lambda_a(\phi_a + i\rho_a)$ with the U(2) generators λ_a ($a = 0, 1, 2, 3$). The usual ground state breaks the chiral symmetry spontaneously, having nonzero chiral condensate ϕ_0. At finite μ_I the pion-condensed phase where $\rho_{1,2}$ are nonzero may be favored. Therefore, we adopt here the following Ansatz:

$$S = \begin{pmatrix} \phi_u & i\rho_1 + \rho_2 \\ i\rho_1 - \rho_2 & \phi_d \end{pmatrix} \qquad (14)$$

with real order parameters ϕ_u, ϕ_d, and $\rho_{1,2}$. Notice that nonzero μ_I explicitly breaks the SU(2) isospin invariance down to U(1) invariance generated by λ_3, and then $\phi_u \neq \phi_d$ in general. Substituting this form into the effective potential (10), we obtain

$$\Omega = \frac{\Sigma^2}{2}(\phi_u^2 + \phi_d^2 + 2|\rho|^2)$$
$$- \frac{1}{2} \log[(\sigma_u + \mu_u)(\sigma_d - \mu_d) + |\rho|^2]$$
$$- \frac{1}{2} \log[(\sigma_u - \mu_u)(\sigma_d + \mu_d) + |\rho|^2]$$
$$- \frac{\gamma}{2} \log[\alpha(\sigma_u \sigma_d + |\rho|^2) + 1]^2, \qquad (15)$$

where $\sigma_f = \phi_f + m$. This model reduces to the one studied in Ref. [8], when the anomaly term is neglected $\gamma\alpha = 0$ as it should. Note that the potential depends on ρ_1 and ρ_2 only through $|\rho|^2 = \rho_1^2 + \rho_2^2$ due to the residual U(1) symmetry. Hereafter, we shall arbitrarily choose the meson condensate such that $\rho_1 = 0$ and $\rho_2 = \rho$, which breaks the U(1) invariance. Nonzero $\rho = (\langle \bar{u}\gamma_5 d \rangle - \langle \bar{d}\gamma_5 u \rangle)/2$ signals the pion condensation.

The saddle point equations with respect to ϕ_u, ϕ_d, and ρ respectively yield

$$\frac{\partial \Omega}{\partial \phi_u} = \Sigma^2 \phi_u - \frac{1}{2}\left[\frac{\sigma_d - \mu_d}{(\sigma_u + \mu_u)(\sigma_d - \mu_d) + \rho^2}\right.$$
$$\left. + \frac{\sigma_d + \mu_d}{(\sigma_u - \mu_u)(\sigma_d + \mu_d) + \rho^2}\right]$$
$$- \frac{\gamma \alpha \sigma_d}{\alpha(\sigma_u \sigma_d + \rho^2) + 1} = 0, \qquad (16)$$

$$\frac{\partial \Omega}{\partial \phi_d} = \Sigma^2 \phi_d - \frac{1}{2}\left[\frac{\sigma_u + \mu_u}{(\sigma_u + \mu_u)(\sigma_d - \mu_d) + \rho^2}\right.$$
$$\left. + \frac{\sigma_u - \mu_u}{(\sigma_u - \mu_u)(\sigma_d + \mu_d) + \rho^2}\right]$$
$$- \frac{\gamma \alpha \sigma_u}{\alpha(\sigma_u \sigma_d + \rho^2) + 1} = 0, \qquad (17)$$

$$\frac{\partial \Omega}{\partial \rho} = 2\Sigma^2 \rho - \frac{1}{2}\left[\frac{2\rho}{(\sigma_u + \mu_u)(\sigma_d - \mu_d) + \rho^2}\right.$$
$$\left. + \frac{2\rho}{(\sigma_u - \mu_u)(\sigma_d + \mu_d) + \rho^2}\right]$$
$$- \frac{2\gamma \alpha \rho}{\alpha(\sigma_u \sigma_d + \rho^2) + 1} = 0. \qquad (18)$$

Let us first classify the solutions with $\rho = 0$. Remember that when $\alpha\gamma = 0$, the chiral condensates ϕ_u and ϕ_d decouple from each other. Thus, in the ideal case of $m = 0$, we have four solutions by making combinations of $\phi_f = 0$ and $\phi_f \neq 0$, depending on the values of μ_f. If $\alpha\gamma \neq 0$, however, the condensate ϕ_d cannot vanish exactly once $\phi_u \neq 0$ because of the flavor mixing, while the trivial solution $\phi_u = \phi_d = 0$ is still intact. Thus, in the chiral limit with $\alpha\gamma \neq 0$, we expect four types of solutions: (i) ordinary phase with broken chiral symmetry, (ii) phase with restored chiral symmetry, (iii) and (iv) phases with nearly vanishing chiral condensate for only one of the flavors, u and d. We numerically find that the transitions between these four phases are of first order, and hence these four phases remain at small $m \neq 0$.

We next consider in what conditions the $\rho \neq 0$ solution appears. To this end, we expand the thermodynamic potential with respect to ρ at the ordinary ground state $\partial \Omega / \partial \phi_{u,d} = 0$ and $\rho = 0$:

$$\Omega(\rho; m, \mu_f) = \Omega_0(m, \mu_f) + \Omega_2(m, \mu_f)\rho^2 + \cdots. \qquad (19)$$

Then one finds the coefficient Ω_2 up to $\mathcal{O}(m, \mu_I^2)$ as

$$\Omega_2 = M_\pi^2 - \frac{2\mu_I^2}{(\phi_0^2 - \mu_q^2)^2}\left(1 + \frac{\mu_q^2}{(\phi_0^2 - \mu_q^2)^2 \Sigma^2}\right)^{-1}, \qquad (20)$$

where ϕ_0 is the scalar condensate at $m = \mu_I = 0$. We see that the finite pion mass $M_\pi^2 = m\Sigma^2/\phi_0$ disfavors the pion condensation, while the finite chemical potential μ_I favors it. From the condition $\Omega_2 = 0$, the critical isospin

chemical potential is found to be $\mu_{Ic}^2 \propto M_\pi^2$ within this leading approximation.[3]

When $m = 0$ *i.e.* $m_\pi^2 = 0$, infinitesimal μ_I selects out the ground state solution of $\phi_u = \phi_d = 0$ and $\rho \neq 0$ among the degenerate vacua. We find that from Eq. (18) the nontrivial solution satisfies the relation

$$\rho^2 = \mu_u \mu_d + \left(\Sigma^2 - \frac{\alpha\gamma}{\alpha\rho^2 + 1}\right)^{-1}. \qquad (21)$$

For $\alpha\gamma = 0$ this recovers the solution of [8]

$$\rho_0^2 = \mu_u \mu_d + \frac{1}{\Sigma^2} = \mu_q^2 - \mu_I^2 + \frac{1}{\Sigma^2}. \qquad (22)$$

In the large μ_I^2 region, $\rho^2 > 0$ solution disappears and the U(1) symmetry is restored. The second-order transition line is given by a hyperbola on the μ_q–μ_I plane, obtained by setting $\rho = 0$ in Eq. (21). This pion-condensed region is enlarged by a factor $(1 - \alpha\gamma/\Sigma^2)^{-1}$ as compared to the case without anomaly.

Before analyzing the ground state solution numerically, we remark here the symmetry of the effective potential (10). First the effective potential is invariant under the respective charge conjugations $\mu_u \rightarrow -\mu_u$ and/or $\mu_d \rightarrow -\mu_d$ when $\rho = 0$. In addition, the effective potential (10) is invariant under $u \leftrightarrow d$. Reflecting these invariant operations, the phase diagram has an eightfold structure on the μ_u–μ_d or μ_q–μ_I plane. Nonzero condensation ρ of the charged pion, however, breaks the respective charge conjugation symmetry leaving only the simultaneous one $(\mu_u, \mu_d) \rightarrow (-\mu_d, -\mu_u)$. Together with the flavor symmetry $u \leftrightarrow d$, a fourfold structure remains in the phase diagram. On the μ_q–μ_I plane, therefore, it is sufficient to investigate the phase diagram in the first quadrant $\mu_q > 0$ and $\mu_I > 0$.

B. Numerical result

In the top panel of Fig. 1, we show the phase diagram on the μ_q–μ_I plane with parameters $\alpha = 0.5$, $\gamma = 1$, $\Sigma = 1$, and $m = 0$. The dotted lines denotes the first-order phase transitions with respect to the scalar condensates ϕ_u and ϕ_d when the possibility of the pion condensation is neglected. In this restricted case, we find around the origin the ordinary phase where ϕ_u and $\phi_d \neq 0$. Allowing the pion condensation, we find that it completely covers the region of the ordinary chirally broken phase and it extends to the larger $|\mu_I|$ region, as shown with the solid line in Fig. 1. Let us look at the small chemical potential region first. The ordinary phase with nonzero $\phi_u = \phi_d$ and $\rho = 0$ and the pion-condensed phases with $\rho \neq 0$ are coexisting along the line $\mu_I = \frac{1}{2}(\mu_u - \mu_d) = 0$ in the chiral limit. With an infinitesimal μ_I, however, the ordinary ground state is totally rotated away to the pion-condensed phase.

---

[3]Note that we use a different notation M_π for the pion mass in this model from the physical one m_π because the physical unit in the ChRM model is not fixed.
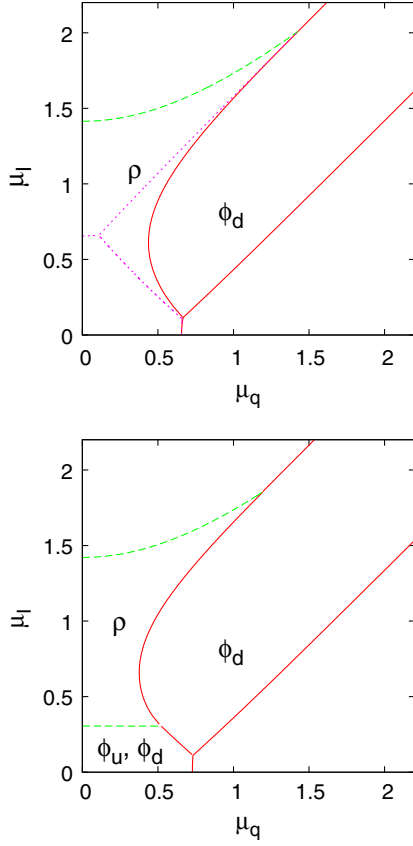
FIG. 1 (color online). Phase diagram for $N_f = 2$ on $\mu_q - \mu_I$ plane in the chiral limit (top) and at $m = 0.1$ (bottom). Parameters are $\alpha = 0.5$, $\gamma = 1$, and $\Sigma = 1$. Nonzero condensates in the respective regions are indicated with the letters ρ and $\phi_{u,d}$. The first (second) order phase boundary is denoted in solid (dashed) lines. For comparison, the phase boundary in the case where the meson condensation is ignored is denoted in dotted line showing the eightfold symmetry.

This behavior was already found in the chiral sigma model [6]. This is to be expected because the ChRM model is similar to the potential term of the chiral sigma model at small chemical potential μ_f and small symmetry breaking m [8]. Next, in the large-μ_f region in Fig. 1, we see that the chiral symmetry restoration occurs. Increasing μ_I with μ_q kept small, we find a second-order phase transition from the pion-condensed phase to the chiral-restored phase. On the other hand, if we increase μ_q along with the fixed μ_I line, we find a first-order phase transition from the pion-condensed phase to the phase where one or both of the chiral condensates ϕ_u and ϕ_d melt away, depending on the size of μ_I. It is remarkable that the phase diagram with $\rho = 0$ reflects the symmetry of $(\mu_q, \mu_I) \leftrightarrow (\mu_I, \mu_q)$ with $(\phi_u, \phi_d) \leftrightarrow (\phi_d, \phi_u)$, while in the real ground state with $\rho \neq 0$, this symmetry no longer exists. As we mentioned, the phase diagram has the symmetry of $(\mu_q, \mu_I) \rightarrow (\pm\mu_q, \pm\mu_I)$.

In the bottom panel of Fig. 1, we show the result with $m = 0.1 \neq 0$. Generally, finite m acts as an external

alignment field for ϕ_u, $\phi_d \neq 0$. So there is a competition between the two alignment fields m and μ_I^2. In a small μ_I region, the finite m wins and the ordinary phase with non-zero ϕ_u and ϕ_d appears pushing the pion-condensed phase aside, as shown in Fig. 1. If μ_I exceeds a critical value proportional to m_π, the pion condensation phase appears. It is estimated from Eq. (20) with our model parameters as $\mu_{Ic} = \sqrt{\phi_0^4 M_\pi^2 / 2} = 0.276$ at $\mu_q = 0$. We here remark the number of the phase transitions in small μ_I region where $\rho = 0$. When μ_q is increased, the system experiences just one phase transition from the ordinary phase with $\phi_u > 0$ and $\phi_d > 0$ to the symmetric phase with $\phi_u \sim 0$ and $\phi_d \sim 0$ if $|\mu_I|$ is sufficiently small. If $|\mu_I|$ is large but still below the critical value, we have two transitions between the ordinary phase and the symmetric phase; e.g., for $\mu_I > 0$, the first one is from the phase of $\phi_u > 0$, $\phi_d > 0$ to $\phi_u \sim 0$, $\phi_d > 0$, and the second is from $\phi_u \sim 0$, $\phi_d > 0$ to $\phi_u \sim 0$, $\phi_d \sim 0$. In the study of the ChRM model without the anomaly effect in [8], a two-step phase transition is found. We find that, even with $\rho = 0$, the anomaly term mixes the ϕ_u and ϕ_d yielding a one-step transition. This mechanism is general and is found in an NJL model study [14]. We expect that this is also the case in QCD. As a result, we have one triple point and two critical end points[4] in the phase diagram shown in the bottom of Fig. 1. (In the $N_f = 3$ case, we will find more triple points and critical end points.) Varying the anomaly parameters α and γ, we have confirmed that the position of the triple point moves toward the larger μ_q and μ_I region as the strength of the flavor mixing is increased.

Finally, we comment on the large μ_I region regarding the possibility of BCS-like condensate. At large μ_I in QCD, large Fermi seas of (e.g.) u quark and d quark are formed, and the attraction between these quarks may form a pionlike Cooper pair [6]. However, since the ChRM model neglects the space-time dimensions, the physics of the Fermi surface does not exist and the superconducting phase is tricky. For possible extensions of the ChRM models to deal with the diquark condensates, see Ref. [30]. In our model without such an extension, we find a simple termination of the pion-condensed phase at large $|\mu_I|$.

V. PHASE DIAGRAM: $N_f = 3$ CASE

A. Effective potential

We explore here the phase structure in the $2 + 1$ flavor case with two mass parameters, $m_u = m_d \equiv m$ and m_s, varying three chemical potentials μ_u, μ_d, and μ_s independently. They are recast to the quark chemical potential μ_q, the isospin chemical potential μ_I, and the hypercharge chemical potential μ_Y defined, respectively, as

---

[4]A critical end point is the point where a critical line is truncated by meeting a first-order phase boundary.

$$\mu_q = \frac{1}{2}(\mu_u + \mu_d), \tag{23}$$

$$\mu_I = \frac{1}{2}(\mu_u - \mu_d), \tag{24}$$

$$\mu_Y = \frac{1}{2}(\mu_u + \mu_d - 2\mu_s). \tag{25}$$

Note that $\mu_Y = \mu_q - \mu_s$ in our convention. When $\mu_I = \mu_Y = 0$, three quark chemical potentials are equal to μ_q. At nonzero μ_I and μ_Y, we allow the possibilities for the pion and kaon condensates in addition to the chiral condensates. We then apply the following Ansatz for the order parameter matrix

$$S = \begin{pmatrix} \phi_u & \rho_{ud} & -\rho_{su} \\ -\rho_{ud} & \phi_d & \rho_{ds} \\ \rho_{su} & -\rho_{ds} & \phi_s \end{pmatrix}, \tag{26}$$

where ϕ_u, ϕ_d, and ϕ_s are the chiral condensates, ρ_{ud} is the pion condensate, and ρ_{su} and ρ_{ds} are the kaon condensates. With this Ansatz, we obtain the effective potential as an function of six order parameters

$$\Omega = \Omega_0 + \Omega_a, \tag{27}$$

where Ω_0 is the potential of the conventional ChRM model [9]

$$\begin{aligned} \Omega_0 = &\frac{\Sigma^2}{2}(\phi_u^2 + \phi_d^2 + \phi_s^2 + 2\rho_{ds}^2 + 2\rho_{su}^2 + 2\rho_{ud}^2) \\ &- \frac{1}{4}\log\{(\sigma_u^2 - \mu_u^2)(\sigma_d^2 - \mu_d^2)(\sigma_s^2 - \mu_s^2) \\ &+ [\rho_{ds}^4(\sigma_u^2 - \mu_u^2) + 2\rho_{ds}^2\rho_{su}^2(\sigma_u\sigma_d - \mu_u\mu_d) \\ &+ 2\rho_{ds}^2(\sigma_u^2 - \mu_u^2)(\sigma_d\sigma_s - \mu_d\mu_s) \\ &+ (\text{cyclic perm. of u, d, s})]\}^2, \end{aligned} \tag{28}$$

and Ω_a is the anomaly part[5]

$$\begin{aligned} \Omega_a = &-\frac{\gamma}{2}\log[\alpha(\sigma_u\sigma_d\sigma_s + \sigma_u\rho_{ds}^2 + \sigma_d\rho_{su}^2 \\ &+ \sigma_s\rho_{ud}^2) + 1]^2. \end{aligned} \tag{29}$$

Because Ω is a function of ρ_{ud}^2, ρ_{ds}^2, and ρ_{su}^2, we always have a trivial solution $\rho_{fg} = 0$ for the saddle point equations. On the other hand, once chiral and/or meson condensates become nonzero, they act as source terms for the other chiral condensates owing to the anomaly term Ω_a, and therefore $\sigma_f = 0$ is no longer a solution.

We confirmed numerically in the ChRM model that two or more meson condensates do not appear in the ground state at the same time. If only one type of the meson condensate ρ_{fg} is nonzero, the Ω_0 part of the potential

becomes a sum of two contributions $\Omega_0 = \Omega_0^{fg}(\rho_{fg}, \phi_f, \phi_g) + \Omega_0^h(\phi_h)$, where Ω_0^{fg} is nothing but the potential of the two-flavor (fg) ChRM model without anomaly, and Ω_0^h corresponds to the single-flavor (h) ChRM model. In spite of this flavor separation, the phase diagram of $N_f = 3$ is different from that of $N_f = 2$ because the anomaly term introduces the coupling among three flavors, and we have a competition between the pion ($fg = ud$) and the kaon ($fg = ds$ or su) condensed phases for being the ground state. Below, we just assume that only one component of the meson condensates becomes nonzero in the meson condensed phase and leave its proof as an open issue.[6]

Preceding the numerical results, let us summarize three key points for qualitative understanding of the phase structure.

(I) *analogy with the chiral sigma model*—As is shown in Ref. [8], the conventional ChRM model for small chemical potentials and quark masses is equivalent to the zero momentum part of the chiral Lagrangian. Hence, the phase structure of the ChRM model in the small chemical potential region must have a similar structure as the chiral sigma model. It is known in the sigma model with $N_f = 3$ that a second-order phase transition occurs from the ordinary chirally broken phase to the pion-condensed phase or the kaon-condensed phase at certain finite μ_I and μ_Y. The critical chemical potential is roughly estimated as $\mu_I \sim m_\pi/2$ and $\mu_Y \sim m_K$ for the pion and kaon condensations, respectively. There is a competition between the pion and kaon-condensed phases for finite μ_I and μ_Y, and the phase transition between the two is found to be first-order. We also remark that the state with two meson condensates having nonzero values can not be even a meta-stable state in this analysis.

(II) *chiral restoration*—In contrast to the chiral sigma model, the ChRM model includes the chiral restoration dynamics, which will result in a new kind of competition of two meson condensed phases in the region at large chemical potential. To illustrate the situation, let us consider the case in the chiral limit, where $\mu_Y > \mu_I > \mu_q = 0$ and the K^0-condensed phase $\rho_{us} \neq 0$ with $\phi_d \neq 0$ is chosen as the ground state. We now further increase μ_Y with μ_q and μ_I fixed. This kaon-condensed phase will simply remain as the ground state in the chiral sigma model. At sufficiently large μ_Y, however, chiral or meson condensates involving the s quark become disfavored and the chiral symmetry in the s-quark sector will presumably be restored. Then there is a possibility for the remaining u and d quarks to form the pion condensate $\rho_{ud} \neq 0$. We thus find a competition between the kaon-condensed phase ($\rho_{us} \neq 0$, $\phi_d \neq 0$) and the pion-condensed phase ($\rho_{ud} \neq 0$, $\phi_s = 0$) at large μ_Y. We will see shortly in this section

---

[5]Consequences of the anomaly mixing between the chiral and diquark condensates are studied in Ref. [31].

[6]We note that coexistence of the p-wave pion and kaon condensates in nuclear matter was studied previously [32].

that the pion-condensed phase is indeed favored at large μ_Y. This competition exists also in the NJL model [12], and we expect that this mechanism is common for the models exhibiting chiral symmetry restoration at large chemical potentials.

(III) *anomaly effect*—Mixing of the order parameters due to the anomaly tends to unify chiral phase transitions into a single one as is seen in the case of $N_f = 2$. In the absence of the meson condensates, the anomaly term Ω_a for $N_f = 3$ reduces to $\log(\alpha\sigma_u\sigma_d\sigma_s + 1)$, which couples three chiral condensates. When one of the chiral condensates melts away, the flavor mixing among the chiral condensates becomes small. With finite meson condensates, however, the anomaly term induces mixing among the chiral and the meson condensates. For example, once the pion condensate is formed $\rho_{ud} \neq 0$ with rotating ϕ_u and ϕ_d away, the mixing term $\sigma_u\sigma_d\sigma_s$ becomes small, but the term $\phi_s\rho_{ud}^2$ in Eq. (29) generates new flavor mixing. Because of this mixing, the chiral and pion condensates tend to vary cooperatively as the chemical potentials change. Furthermore, the anomaly term makes the ground state with nonzero ϕ_s and ρ_{ud} condensates more stable as the term appears with a minus sign in the effective potential, which results in the extension of the meson condensed phase compared to the case without anomaly.

B. Numerical result

We calculated the phase diagram with model parameters $\Sigma = 1$, $\alpha = 0.5$, and $\gamma = 1$ in the chiral limit $m_u = m_d = m_s = 0$ as well as at finite quark masses $m_u = m_d = 0.02$ and $m_s = 0.1$. We show the phase diagram on the $\mu_I-\mu_Y$ plane with $\mu_q = 0$, the $\mu_q-\mu_I$ plane with $\mu_Y = 0$, and the $\mu_q-\mu_Y$ plane with $\mu_I = 0$.

1. $\mu_I-\mu_Y$ plane

We first present the phase diagram on the $\mu_I-\mu_Y$ plane with zero quark chemical potential $\mu_q = 0$ in the chiral limit (top) and at finite quark masses (bottom) in Fig. 2. Note that the effective potential has the symmetry of $\mu_Y \leftrightarrow -\mu_Y$ and, moreover, $\mu_I \leftrightarrow -\mu_I$ if we change u and d flavors simultaneously. We then present the result only in the first quadrant.

Let us first focus on the case in the chiral limit. In the small chemical potential region, we find the pion and kaon-condensed phases. These two phases are separated by the first-order phase transition line $\mu_I = \mu_Y$; the pion-condensed phase appears when $\mu_I > \mu_Y$ and otherwise the kaon condenses. This is also found in the chiral sigma model [7]. When chemical potentials are increased, we find that the regions of two mesonic phases are exchanged on the diagram; the pion-condensed phase appears when $\mu_I < \mu_Y$ and otherwise the kaon condenses. As already explained, this peculiar behavior is triggered by the chiral restoration; these meson condensed phases at the larger chemical potentials are accompanied by the melting of the
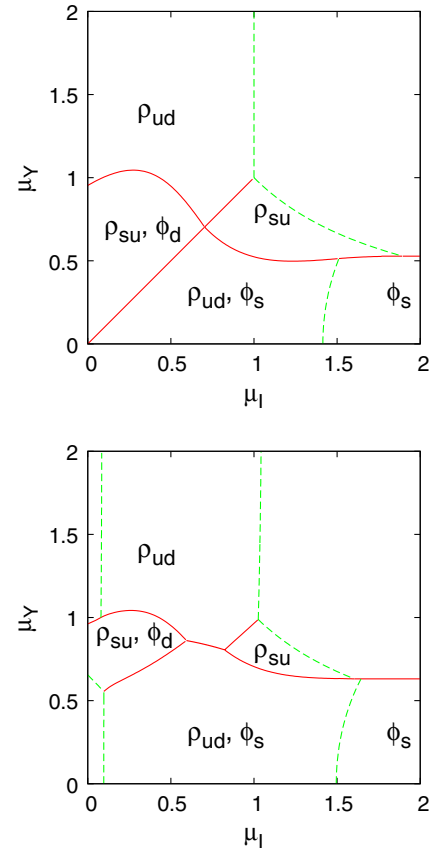

FIG. 2 (color online). Phase diagram for $N_f = 3$ on $\mu_I-\mu_Y$ plane with $\mu_q = 0$ in the chiral limit (top) and with nonzero quark masses $m_u = m_d = 0.02$, $m_s = 0.1$ (bottom). In the bottom panel, the lower (upper) vertical narrow area represents the phase with nonzero ϕ_u, ϕ_d, and ϕ_s (ϕ_u and ϕ_d). Other parameters and notations are the same as in Fig. 1.

chiral condensate of the remaining flavor. When μ_Y is further increased at small μ_I, the pion-condensed phase continues indefinitely because ρ_{ud} becomes insensitive to μ_Y once ϕ_s disappears. On the other hand, ρ_{ud} continuously vanishes at some point as μ_I increases because ρ_{ud}, which has the isospin charge, is affected by μ_I, whereas nonzero chiral condensate ϕ_s survives irrespective of μ_I for small μ_Y because it has no isospin.

Without the anomaly term, the vertical straight line of the second-order transition boundary seen in the large μ_Y region in Fig. 2 would extend down to the μ_I axis. This is because the effective potential without anomaly Ω_0 becomes the sum of two contributions, the ϕ_s part and the part involving ϕ_u, ϕ_d, and ρ_{ud}, as mentioned before, unless the kaon condensates have finite values. By comparison, we see that the anomaly coupling between ϕ_s and ρ_{ud} makes the pion-condensed phase more stable and extended to larger μ_I region.

When quark masses are set to nonzero, the phase diagram receives two qualitative modifications. One is the appearance of the chiral condensed phase without any

meson condensate at small chemical potentials. This is the same result as in the chiral sigma model. The other is the configuration change of the four meson condensed phases. We find that the pion-condensed phase extends from zero μ_Y to large μ_Y, cutting the two kaon-condensed phases apart. This is because the chiral condensate ϕ_s is more favored for $m_s > m_u = m_d$ and the kaon-condensed phases shrink. In the extended pion-condensed phase, we find a first-order phase transition in ϕ_s, which creates a small gap in ρ_{ud}, too.

2. μ_q–μ_I plane

We next show the phase diagram on the μ_q–μ_I plane with $\mu_Y = 0$ in Fig. 3. In this case, the effective potential is symmetric in $\mu_q \leftrightarrow -\mu_q$ and in $\mu_I \leftrightarrow -\mu_I$ with exchange of the u and d quarks. We present the phase diagram again only in the first quadrant.

Let us focus on the case in the chiral limit (top panel of Fig. 3). With infinitesimal μ_I, the ground state becomes the pion-condensed phase. Unexpectedly, however, we find that a kaon-condensed phase appears in the region where
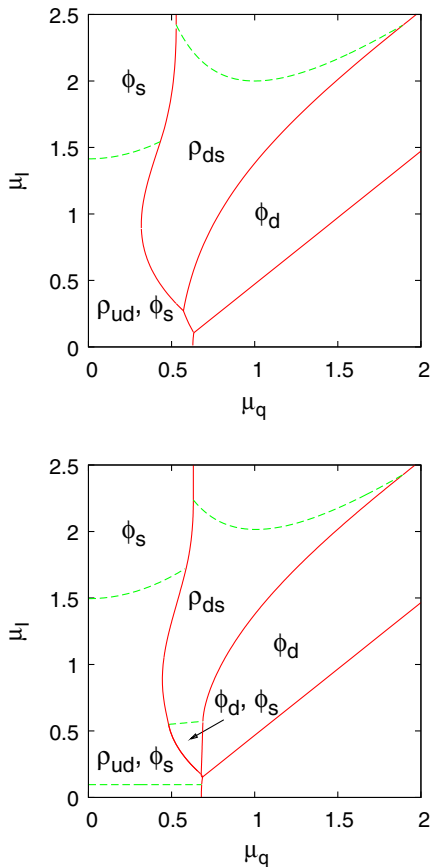

FIG. 3 (color online).   Phase diagram for $N_f = 3$ on μ_q–μ_I plane with $\mu_Y = 0$ in the chiral limit (top) and with nonzero quark masses (bottom). In the bottom panel, the horizontal narrow area is the phase with nonzero ϕ_u, ϕ_d, and ϕ_s. Parameters and notations are the same as in Fig. 2.

μ_u becomes largest among three chemical potentials. This phase was not predicted in the chiral Lagrangian analysis. In this phase, the u-quark chiral condensate melts away $\phi_u \sim 0$, and the remaining d and s quarks form the kaon condensate $\rho_{ds} \neq 0$. Note that, because $m_K = 0$, infinitesimal difference between μ_d and μ_s makes the kaon-condensed phase more stable than the chirally broken phase without a meson condensate.

The pion and kaon-condensed phases vanish continuously at large μ_I, respectively, to the phases with ϕ_s and without any condensate. The kaon-condensed phase extends to a larger μ_I region than the pion-condensed phase. This may be understood from the fact that the pion condensate with isospin charge 1 is twice as sensitive to μ_I as the kaon condensate with isospin $1/2$.

With finite quark masses, we observe that two new phases are added, as is seen in the bottom panel of Fig. 3. The ordinary chirally broken phase appears in the small μ_I and μ_q region due to finite m_π, while finite m_K changes lower chemical potential part of the kaon-condensed region into the chiral condensed phase with nonzero ϕ_d and ϕ_s. These two chiral condensed phases show the second-order phase transitions to the meson condensed phases at larger μ_I, which is consistent with the chiral Lagrangian analysis [7]. At small μ_I, we find a single transition from the broken to the symmetric phase along the μ_q axis, owing to the anomaly term.

It would be instructive to compare this phase diagram to that of $N_f = 2$ on the μ_q–μ_I plane. Although the phase diagrams are drawn in the same chemical potential space, inclusion of the third quark flavor changes the phase diagram drastically resulting in a new phase with the kaon condensation. If we take a limit of $m_s \to \infty$ in the $N_f = 3$ phase diagram, the s quark should decouple and the s-quark and kaon condensates disappear. This makes the phase diagram reduce to that of the $N_f = 2$ case.

3. μ_q–μ_Y plane

Finally, we address the phase diagram on the μ_q–μ_Y plane with $\mu_I = 0$. In Fig. 4, we present the phase diagram in the chiral limit (top panel) and with finite quark masses (bottom panel). The effective potential is unchanged under the simultaneous exchanges of $\mu_q \leftrightarrow -\mu_q$ and $\mu_Y \leftrightarrow -\mu_Y$. Hence, we restrict the phase diagrams in $\mu_Y > 0$ region. The formation of the kaon condensate breaks the SU(2) isospin symmetry spontaneously. We choose arbitrarily the K_0-condensed phase ($\rho_{ds} \neq 0$) as the meson condensed ground state. Note that no pion-condensed phase appears in this diagram since we have set $|\mu_I| = 0 \leq m_\pi$.

In the chiral limit, the chiral and kaon (pion as well) condensed phases are degenerated at $\mu_q = \mu_Y = 0$. With infinitesimal μ_Y, the ground state becomes the kaon-condensed phase, and therefore the isospin symmetry is broken spontaneously. Assuming the alignment by
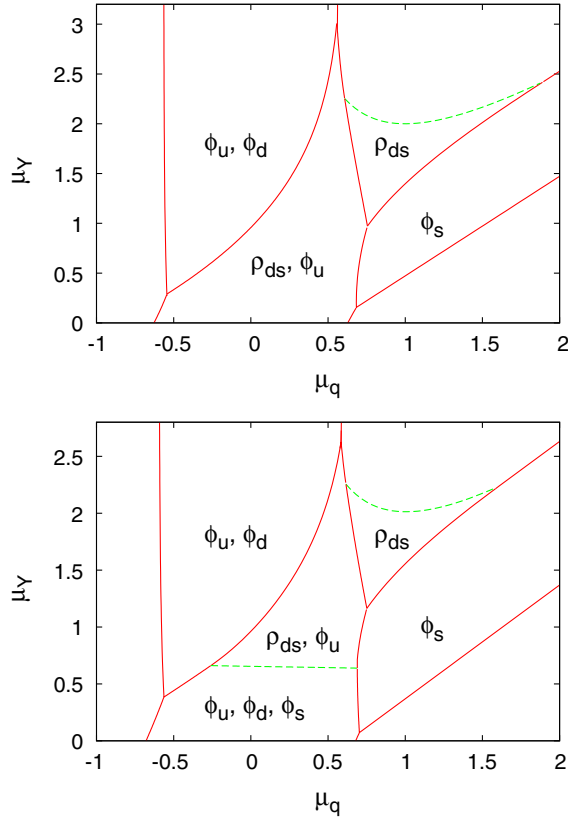
FIG. 4 (color online).   Phase diagram for $N_f = 3$ on μ_q–μ_Y plane with $\mu_I = 0$ in the chiral limit (top) and with nonzero quark masses (bottom). Parameters and notations are the same as in Fig. 2.

infinitesimal negative μ_I, the chiral condensed state is completely rotated into the K^0 condensed state, where $\phi_d = \phi_s = 0$ and $\rho_{ds} \neq 0$, but the u-quark chiral condensate remains finite $\phi_u \neq 0$. When μ_q is increased with $\mu_Y = 0$, two order parameters ρ_{ds} and ϕ_u disappear at the same time at a critical value. Without the anomaly effect this phase transition would occur in two steps.

We note that there is a first-order phase boundary inside of the the kaon-condensed phase $\rho_{ds} \neq 0$. Across this line, ϕ_u jumps from a nonzero value to zero and ρ_{ds} changes also its value discontinuously. At one end of this line, we find a triple point where the two kaon-condensed phases and the $\phi_s \neq 0$ phase coexist. At the other end, we find a critical end point where two kaon-condensed phases and the symmetric phase meet.

Let us consider the finite mass effect. Because of the finite m_K, there appears the ordinary chirally broken phase in the small chemical potential region. The phase transition to the kaon-condensed phase is of second order. Along the μ_q axis, we find the phase transition from the chiral condensed phase to the symmetric phase occurs in one step. The threshold μ_Y for the two-step phase transition is relatively small compared to the corresponding value of μ_I found in the μ_q–μ_I plane (see Fig. 3).

This can be understood as follows: note that without the flavor mixing, the first-order transitions along the μ_q axis would occur at different values of μ_q when the quark masses are different. The $U(1)_A$ anomaly mixing acts to bind them together, and there is a critical value for the anomaly strength above which the phase transitions occur in one step along the μ_q axis. The larger mass difference between u, d quarks and s quark makes this binding of the chiral transition more fragile against the external field μ_Y. This is the reason why we have a smaller threshold value of μ_Y compared to the threshold value of μ_I.

With the mass parameters $m_u = m_d = 0.02$ and $m_s = 0.1$ used in Fig. 4, the threshold value is found to be $\alpha_c = 0.279\ldots$ when $\gamma = 1$ is fixed. In Fig. 4, $\alpha = 0.5 > \alpha_c$, and we see the one-step phase transition along the μ_q axis.

VI. SUMMARY

We have investigated the phase structure of the ChRM model with 2 and 3 flavors on the plane of the quark chemical potentials, including the effects of anomaly. Different chemical potentials for different flavors are realized in general situations because of the quark mass differences and electric neutrality, and the chiral condensates have also different values there. Moreover, when the chemical potential difference, which is flavor nonsinglet, becomes large and comparable to the pseudoscalar meson masses, we have a phase transition to a meson condensed phase. We obtained a complex structure of the phase diagram with various orderings at first sight. Nevertheless, we can understand the diagram qualitatively based on the following three observations.

The first point is the similarity to the chiral Lagrangian analysis, which explains the phase structure well below the chiral restoration. In the chiral limit for $N_f = 2$, the chiral condensed phase and the pion-condensed phase are degenerated at $\mu_I = 0$, and an infinitesimal μ_I rotates the chiral condensates into the pion condensate. With finite quark masses the chiral condensed phase survives up to $\mu_I \sim m_\pi/2$, and we find a second-order phase transition to the pion-condensed phase. In the $N_f = 3$ case, a similar behavior is also found for meson condensations, but in addition we found a new competition between the pion and kaon-condensed phases, bounded by a first-order phase transition.

The second point concerns the chiral restoration, whose effect is not included in the chiral Lagrangian analysis. For $N_f = 2$ and 3, we found that the pion and kaon condensates disappear continuously at large μ_I and μ_Y, respectively, while the phase transitions along the μ_q axis are first order. The chiral restoration effect explains the peculiar appearance of the pion and the kaon-condensed phases in the phase diagram for $N_f = 3$. In the chiral Lagrangian analysis, the pion condensation is always favored if $\mu_I > \mu_Y$. However, when μ_I is further increased, the chiral

restoration for u quark should occur and the pion conden-sation melts away. Then, the kaon condensation will be formed if the difference between μ_d and μ_s is larger than a certain critical value characterized by m_K. This argument also holds in the situation where $\mu_I < \mu_Y$ with exchanging the pion and kaon condensates. This is a remarkable in-version of the pion and kaon condensation at high μ_I or μ_Y. Note that the argument does not depend on the details of the ChRM model. The same inversion may be found in other models which incorporate the chiral restoration dynamics, and therefore one may expect this also in QCD.

The third point is about the anomaly effect. The most important effect is the mixing of the condensates. For $N_f = 2$ with finite quark masses, we find a single phase transition from the chiral condensed phase to the symmet-ric phase along the μ_q axis. Without the flavor mixing, the u and d quarks would show the chiral transitions indepen-dently at finite μ_I. But these two phase transitions coalesce into a single transition via the flavor mixing term due to the $U(1)_A$ anomaly. There is the threshold μ_I for two-step phase transition, which becomes large if the anomaly parameters are increased.

In the case of $N_f = 3$, the anomaly effect induces the mixing among not only the chiral condensates but also the meson condensates, which makes likely that the meson condensate and the chiral condensate of the remaining flavor show the discontinuity simultaneously as the chemi-cal potentials are varied. In the mean-field models without the anomaly effect, where the flavor mixing is missing, the chiral phase transitions can happen in multi steps for finite

μ_I and/or μ_Y even when the quarks have an equal mass. We expect that the chiral condensates are strongly corre-lated in QCD because of the anomaly mixing as well as the dynamics beyond the mean field, and it is unlikely to have the multistep chiral restoration in QCD when μ_q is in-creased with μ_I and μ_Y being not too large. For large μ_I and/or μ_Y, however, there remains a possibility for chiral restoration to occur in multi steps, as shown in our model study.

The ChRM model, which discards the space-time dynamics but keeps the chiral symmetry only, is certainly a simplified model for QCD and will provide at most qualitative features of the QCD phase diagram. We have studied the response of the condensates to the chemical potentials using this ChRM model with the $U(1)_A$ anomaly and found interesting interplay between the chiral and meson condensates as well as the importance of the $U(1)_A$ anomaly effects. It will be intriguing to confirm and elaborate the findings of this study by employing other dynamic and microscopic models for QCD and direct simulations.

[1] K. Rajagopal and F. Wilczek, *At the Frontier of Particle Physics: Handbook of QCD*, edited by M. Shifman (World Scientific, Singapore, 2001).

[2] K. Fukushima and T. Hatsuda, arXiv:1005.4814.

[3] See, for example, T. Kunihiro, T. Muto, R. Tamagaki, T. Tatsumi, and T. Takatsuka, Prog. Theor. Phys. Suppl. **112**, 1 (1993).

[4] For a recent review, M. G. Alford, A. Schmitt, K. Rajagopal, and T. Schafer, Rev. Mod. Phys. **80**, 1455 (2008).

[5] E. Nakano and T. Tatsumi, Phys. Rev. D **71**, 114006 (2005); D. Nickel, Phys. Rev. Lett. **103**, 072301 (2009); Phys. Rev. D **80**, 074025 (2009).

[6] D. T. Son and M. A. Stephanov, Phys. Rev. Lett. **86**, 592 (2001).

[7] J. B. Kogut and D. Toublan, Phys. Rev. D **64**, 034007 (2001).

[8] B. Klein, D. Toublan, and J. J. M. Verbaarschot, Phys. Rev. D **68**, 014009 (2003).

[9] R. Arai and N. Yoshinaga, Phys. Rev. D **78**, 094014 (2008).

[10] R. Arai and N. Yoshinaga, Phys. Rev. D **80**, 017501 (2009).

[11] A. Barducci, R. Casalbuoni, G. Pettini, and L. Ravagli, Phys. Rev. D **69**, 096004 (2004).

[12] A. Barducci, R. Casalbuoni, G. Pettini, and L. Ravagli, Phys. Rev. D **71**, 016011 (2005).

[13] D. Toublan and J. B. Kogut, Phys. Lett. B **564**, 212 (2003).

[14] M. Frank, M. Buballa, and M. Oertel, Phys. Lett. B **562**, 221 (2003).

[15] M. Kobayashi and T. Maskawa, Prog. Theor. Phys. **44**, 1422 (1970); M. Kobayashi, H. Kondo, and T. Maskawa, Prog. Theor. Phys. **45**, 1955 (1971).

[16] G. 't Hooft, Phys. Rep. **142**, 357 (1986).

[17] R. D. Pisarski and F. Wilczek, Phys. Rev. D **29**, 338 (1984).

[18] T. Sano, H. Fujii, and M. Ohtani, Phys. Rev. D **80**, 034007 (2009).

[19] H. Fujii and T. Sano, Phys. Rev. D **81**, 037502 (2010).

[20] L. y. He, M. Jin, and P. f. Zhuang, Phys. Rev. D **71**, 116001 (2005).

[21] A. Barducci, R. Casalbuoni, G. Pettini, and L. Ravagli, Phys. Rev. D **72**, 056002 (2005).

[22] T. Schafer, D. T. Son, M. A. Stephanov, D. Toublan, and J. J. M. Verbaarschot, Phys. Lett. B **522**, 67 (2001).

[23] Y. Nambu, Soryushiron kenkyu **105**, D24 (2002); J. Stat. Phys. **115**, 7 (2004).

[24] E. V. Shuryak and J. J. M. Verbaarschot, Nucl. Phys. A **560**, 306 (1993); A. D. Jackson and J. J. M. Verbaarschot, Phys. Rev. D **53**, 7223 (1996); T. Wettig, A. Schäfer, and H. A. Weidenmüller, Phys. Lett. B **367**, 28 (1996); **374**, 362(E) (1996); for review, J. J. M. Verbaarschot and T. Wettig, Annu. Rev. Nucl. Part. Sci. **50**, 343 (2000).

[25] A. M. Halasz, A. D. Jackson, R. E. Shrock, M. A. Stephanov, and J. J. M. Verbaarschot, Phys. Rev. D **58**, 096007 (1998).

[26] T. Banks and A. Casher, Nucl. Phys. **B169**, 103 (1980).

[27] M. Ohtani, C. Lehner, T. Wettig, and T. Hatsuda, Mod. Phys. Lett. A **23**, 2465 (2008).

[28] C. Lehner, M. Ohtani, J. J. M. Verbaarschot, and T. Wettig, Phys. Rev. D **79**, 074016 (2009).

[29] R. A. Janik, M. A. Nowak, and I. Zahed, Phys. Lett. B **392**, 155 (1997).

[30] B. Vanderheyden and A. D. Jackson, Phys. Rev. D **61**, 076004 (2000); **62**, 094010 (2000); S. Pepin and A. Schafer, Eur. Phys. J. A **10**, 303 (2001); B. Vanderheyden and A. D. Jackson, Phys. Rev. D **72**, 016003 (2005).

[31] T. Hatsuda, M. Tachibana, N. Yamamoto, and G. Baym, Phys. Rev. Lett. **97**, 122001 (2006).

[32] T. Muto, Prog. Theor. Phys. Suppl. **153**, 174 (2004).